Journal of Polymers and the Environment
https://doi.org/10.1007/s10924-024-03262-0

ORIGINAL PAPER

Influence of Biochar on the Properties of Antibacterial PBAT/Carvacrol Films

Francesco Lopresti[1] · Luigi Botta[1] · Giulia Pernice[1] · Giuliana Garofalo[2] · Raimondo Gaglio[2]

Accepted: 23 March 2024

Abstract
In recent years, there has been an increasing interest in antibacterial biopolymeric films. Among the different approaches for tuning the release kinetic of antibacterial compounds, the use of natural fillers allows for this purpose while optimizing the processability and the mechanical properties of the products. In this work, the effect of three different concentrations of biochar (BC) was investigated on the morphological, rheological, mechanical, and thermal properties of Polybutylene adipate terephthalate/Carvacrol/BC (PBAT/CV/BC) ternary biocomposites. The films were fabricated by means of melt mixing and compression molding and compared to PBAT/BC samples. The carvacrol kinetic release was evaluated as a function of the BC concentration in the ternary system. Results highlighted that BC allows tuning the properties of PBAT and of PBAT/CV samples and modifying the release kinetic of CV. Finally, the antimicrobial analysis revealed that PBAT/CV films exhibited excellent antimicrobial properties against *Escherichia coli, Listeria monocytogenes, Salmonella Enteritidis, and Staphylococcus aureus.*

Keywords Biocomposites · PBAT · Biochar · Carvacrol · Antibacterial properties

Introduction

Bacterial infections are persistent and noteworthy challenges in food and biomedical industries [1]. In general, the conventional use of antibiotics or preservatives is a suitable approach to avoid and/or mitigate bacterial proliferation and infections. However, in the frame of a constant bacterial evolution and drug resistance phenomena, the research and development of novel biopolymeric materials able to control the release of antibacterial compounds are in continuous advance [2, 3]. In this context, antimicrobial additives from natural sources, including plant essential oils, are a promising alternative for food and biomedical industries due to their availability, low toxicity, and sustainability [4]. In this context, carvacrol (CV) is a promising bactericidal compound widely explored as additive for biopolymeric matrices [5].

Biodegradable polymers, including poly(butylene adipate terephthalate) (PBAT) [6], thermoplastic starch [7], and poly(lactic acid) [8] are considered suitable polymeric matrices for antibacterial materials development. In particular, PBAT is a fully biodegradable aromatic copolyester with good ductility and a potential alternative to polyolefin-based materials [9] that can be applied to many fields such as shopping bags, garbage bags, cutlery, and mulch film [10]. PBAT was often combined with inorganic nanoparticles [6, 11, 12] or essential oils [13–16] to develop antibacterial devices for active food packaging or biomedical applications [17].

However, the high melt viscosity, low crystallization rate, low tensile strength, and high cost currently restrict PBAT processability and industrial applications [9]. To overcome these drawbacks, PBAT is typically mixed with solid particles to make high-performance composite materials [9]. Several kinds of particles have been proposed as fillers for PBAT aiming at producing biodegradable materials with enhanced performances including lignin [18], silica [19], and cellulose [20]. Recently, biochar (BC) has been considered one of the most promising eco-friendly fillers for sustainable composites fabrication [21]. BC is

✉ Luigi Botta
luigi.botta@unipa.it

[1] Department of Engineering, RU INSTM, University of Palermo, Viale delle Scienze, Palermo 90128, Italy

[2] Department of Agricultural, Food and Forest Sciences, University of Palermo, Viale delle Scienze 4, Palermo 90128, Italy

a high carbon-content material produced by pyrolysis of biomass and has been extensively studied as a filler material for polymers [22]. In most of the existing research, the incorporation of BC into polyesters has been considered as a method for enhancing the mechanical properties of these polymers [21]. In particular, the use of BC for the fabrication of PBAT-based composites showed several interesting improvements in terms of chemical stability and mechanical improvements [23, 24].

However, the type and concentration of filler in ternary antimicrobial biocomposites can also affect the controlled release of the antibacterial compound [25–28].

In this work, three different concentrations of BC were used to prepare ternary PBAT/CV/BC biocomposite films by means of melt mixing and compression molding. The morphological, rheological, mechanical, and thermal properties of PBAT/CV/BC films were evaluated and compared to binary PBAT/BC composites with the same BC parts per hundred of resin (PHR). Moreover, the CV kinetic release was evaluated and modeled through a power law equation as a function of the BC concentration in the ternary systems. Finally, the antimicrobial activity of all the materials containing CV was tested in vitro against the main food-borne pathogenic bacteria.

Materials and Methods

Materials

PBAT (BASF, Ecoflex® F Blend C1200, Germany) in pellet form was used as raw polymer matrix. According to the supplier, it is a biodegradable, statistical, aliphatic-aromatic copolyester based on the monomers 1.4-butanediol, adipic acid, and terephthalic acid in the polymer chain. Its mass density is 1.25–1.27 g/cm^3, with a melting point at 110–120 °C, and melt flow rate (MFR) at 190 °C in the range 2.5–4.5 g/10 min. The monoterpenoid phenol Carvacrol (liquid state, purity ≥ 98%), was purchased from Sigma Aldrich (Munich, Germany). The biochar used in this work is a commercial food grade (E153) supplied by Special Ingredients (Savona, Italy) as an ultrafine powder obtained by pyrolysis of coconut husk.

Table 1 Formulations in parts per hundred of resin of the PBAT-based samples

Sample	PBAT [PHR]	Biochar [PHR]	CV [PHR]
PBAT	100	0	0
PBAT/BC_5	100	5	0
PBAT/BC_10	100	10	0
PBAT/BC_20	100	20	0
PBAT/CV	100	0	20
PBAT/CV/BC_5	100	5	20
PBAT/CV/BC_10	100	10	20
PBAT/CV/BC_20	100	20	20

Film Preparation

PBAT was melt mixed with BC (5, 10, and 20 PHR) and/or CV (20 PHR), resulting in the PHR composition reported in Table 1.

Before processing, PBAT and BC were vacuum-dried at 70 °C for 4 h and at 80 °C for 12 h, respectively.

All the samples were processed by means of a Brabender laboratory mixer (Brabender, model PLE330, Duisburg, Germany) equipped with a mixing chamber of 50 cc set at 170 °C and 60 rpm. The mixing time was 5 min for PBAT and PBAT/BC samples since it was the minimum time required to obtain a plateau of the torque value during mixing. The PBAT/CV/BC mixtures were prepared by melt mixing PBAT and BC for 4 min and then adding CV for the last minute of mixing in order to minimize the evaporation of the compound, according to our previous works [29, 30]. The concentration of 20 PHR for CV was chosen according to our previous work demonstrating its efficacy at this concentration [30]. The PBAT-based samples were then collected and quenched in liquid nitrogen aiming at reducing the CV evaporation after processing.

Films of pure PBAT or PBAT/BC and PBAT/CV/BC biocomposites were prepared using a 15 cm × 15 cm × 0.2 mm height square mold in a Carver laboratory press equipped with water cooling plates (Carver Inc., Wabash, USA) set at 170 °C. The materials were preheated for 2 min in the hot-press and then pressed at 140 bar for 3 min. Then the heating flow in the plates was turned off and cooling water at 15 °C was flow within the plates for 7 min, needed to reach 35 °C, before removing the samples. All the prepared films were stored at 4 °C and characterized within 24 h of fabrication.

Characterizations

Morphological Analysis

Morphology of BC particles, PBAT, PBAT/BC, and PBAT/CV/BC films was observed through scanning electron microscopy (SEM) model Quanta 200 F (FEI, Hillsboro, OR, USA) with the voltage set at 20 kV. SEM micrographs of PBAT-based materials were acquired from samples fractured in liquid nitrogen and gold-sputtered for 90 s. The size of the BC particles was measured from the SEM micrographs using ImageJ software.

Rheological Analysis

The dynamic rheological measurements were performed by using a plate-plate rotational rheometer (ARES G2, TA instruments, New Castle, DE, USA) equipped with a parallel-plate geometry (plate diameter = 25 mm; gap = 1 mm). The instrument has been set to operate at 170 °C in air atmosphere and frequency sweep mode in the range 0.1–100 rad/sec with a strain of 5%. The tests were performed in triplicate.

Mechanical Analysis

The mechanical tensile tests were measured according to ASTM D882 by means of a universal testing machine (UTM) model Instron 3365 (Instron, Norwood, MA, USA). Rectangular specimens (10 × 100 mm) were fixed to the UTM gauges distant 50 mm from each other. Before each test, the actual thickness of the sample was measured by using dial gauges. The measurements were performed at a displacement rate of 100 mm/min. The mechanical properties obtained from the resulting stress-strain curves were calculated as the average of 7 tests, with an adequate reproducibility ± 7%. Additionally, as per ASTM D882 guidelines, separate specimens were tested to determine the tensile modulus. In this case a displacement rate of 1 mm/min was adopted.

Differential Scanning Calorimetry

The calorimetric properties of the materials were studied by using a Differential Scanning Calorimeter (DSC) model DSC131 (Setaram Instrumentation, Caluire, France) equipped with a chiller. PBAT-based film fragments with approximately the same weight (~ 10 mg) were sealed in aluminum pans. The analysis was carried out with one cycle of heating from 0 °C to 200 °C, a cooling cycle from 200 °C to 0 °C, and a second heating cycle from 0 °C to 200 °C. All the cycles were conducted at 10 °C/min under nitrogen flow. The crystallinity of PBAT samples was evaluated according to Eq. 1:

$$\chi_c\,(\%) = \frac{\Delta \mathrm{H_m}}{\Delta \mathrm{H^0_{PBAT}} \times \mathrm{X_{PBAT}}} \times 100 \quad (1)$$

where ΔH_m is the melting enthalpy valued by the calorimeter during the second heating scan; X_{PBAT} represents the PBAT weight fraction and ΔH^0_{PBAT} represents the melting enthalpy of 100% crystalline PBAT (114 J/g [17]). The values were calculated as the average of five measurements (data reproducibility: ±7%).

Water Contact Angle Measurements

The static contact angles test was performed using an FTA 1000 (First Ten Ångstroms, Cambridge, UK) instrument using distilled water (DW) as fluid. In particular, a droplet of DW (~ 4 µL) was dropped on the film, and the images were taken after 10 s from the DW deposition. At least 7 spots of each sample were measured, and the average value was taken.

Carvacrol Release Kinetics

The release curves of CV as a function of time from PBAT/CV/BC composites were evaluated in distilled water at 4 °C using a UV-Vis spectrophotometer (model Specord 252 spectrophotometer, Analytik Jena, Jena, Germany) monitoring the characteristic peak of CV at 273 nm [8]. This temperature was chosen to imitate a potential working condition of the films as active food packaging for food stored in domestic fridges. The calibration line correlating the absorbance and the CV concentration (mg/L) was created by measuring the absorbance of CV/water mixtures at different concentrations from 1 to 50 mg/L of CV, much lower than CV solubility limit in water that is between 750 mg/L [31] and 960 mg/L [32]. PBAT/CV/BC films were cut in rectangles of 10 × 3 cm × 0.2 mm (weight ~ 0.75 g) and dipped in a reservoir containing 10 mL of distilled water, cooled at 4 °C and gently shaken using an orbital laboratory shaker at 100 rpm (Lab Companion, model OS 4000). For each time point, the UV-Vis absorbance of the medium was evaluated and the sample was moved from its reservoir to another one containing 10 mL of fresh distilled water, pre-cooled at 4 °C. This approach was used to avoid misleading results ascribable to the CV evaporation from the medium during the storage and to maintain the concentration of the compound lower than 20% of the solubility limit during the test, according to [33]. The release curves represent the cumulative release of CV calculated by serially adding the CV amount released after each time point. Three samples of each material were analyzed and the average value was reported.

FTIR-ATR Analysis

FTIR-ATR spectra were obtained by using a Spectrum One spectrometer (PerkinElmer Inc., Wellesley, MA, USA) set to perform 16 scans in the range of 4000–400 cm^{-1} with a resolution equal to 4 cm^{-1}.

Bacterial Strains

In order to evaluate the antibacterial properties of biocomposite PBAT films containing CV and 0, 5, 10, and 20% of BC, four bacterial strains belonging to the American Type Culture Collection (ATCC) were used as indicators of microorganisms (sensitive to antimicrobial compounds). In particular, two Gram-positive (*Listeria monocytogenes* ATCC19114 and *Staphylococcus aureus* ATCC33862) and two Gram-negative (*Escherichia coli* ATCC25922 and *Salmonella* Enteritidis ATCC13076) bacteria were chosen as representative of the main food-borne bacterial pathogens. All bacteria were reactivated in Brain Heart Infusion (BHI) broth (Condalab, Madrid, Spain) incubated at 37 °C for 24 h.

Evaluation of Antibacterial Properties

Biocomposite PBAT films were evaluated in vitro for antibacterial properties following the approach reported by Lopresti et al. (2022). Briefly, the washed cells of the four indicator strains were inoculated at the final concentration of 10^6 CFU/mL into 20 mL volume sterile cups (Biogenerica Srl, Pedara, Italy) containing 6 mL of sterile saline solution [NaCl 0.9% (w/v)] and 2 discs (2-cm diameter) of each material. The cups were incubated at 37 °C and the antibacterial activity was evaluated soon after inoculation (0 d) and after 1 and 3 d of incubation. The cell suspensions were firstly serially diluted (Health Canada, 2015) and then spread plated on *E. coli*-Coliforms Chromogenic Medium (CHROMagar™) (Condolab, Madrid, Spain) to enumerate the residual *E.coli*, on *Listeria* Selective Agar Base (LSAB) supplemented with SR0140E (Oxford) for *L. monocytogenes*, on Hektoen Enteric Agar (HEA) (Microbiol Diagnostici, Uta, Italy) for *S.* Enteritidis; and on Baird Parker (BP) added with rabbit plasma fibrinogen (RPF) (Oxoid) for *St. aureus*. CHROMagar™, LSAB, and HEA were incubated aerobically at 37 °C for 24 h, while BP was incubated aerobically at 37 °C for 48 h. Plate counts were performed in duplicate.

Statistical Analysis

Microbiological data were subjected to One-Way Variance Analysis (ANOVA) using XLStat software version 7.5.2 for Excel (Addinsoft, NY, USA) and the differences between mean were determined by Tukey's test at $p < 0.05$.

Results and Discussion

Morphology of PBAT-Based Composites Films

SEM images reported in Fig. 1 were carried out in order to investigate the morphology of the BC microparticles.

Raw coconut husk usually shows a fibrous structure and high lignin content [34]. Due to the pyrolysis process, it is no longer possible to identify the original lignocellulosic structure. Instead, an irregular porous structure and a variable granulometry can be observed, with particle dimensions ranging from 5 to 40 µm, according to ImageJ analysis.

The SEM images of the fractured surfaces of the PBAT/BC (Fig. 2A-D) and PBAT/CV/BC (Fig. 2E-H) composites suggest the good dispersion of the BC particles in the PBAT matrix.

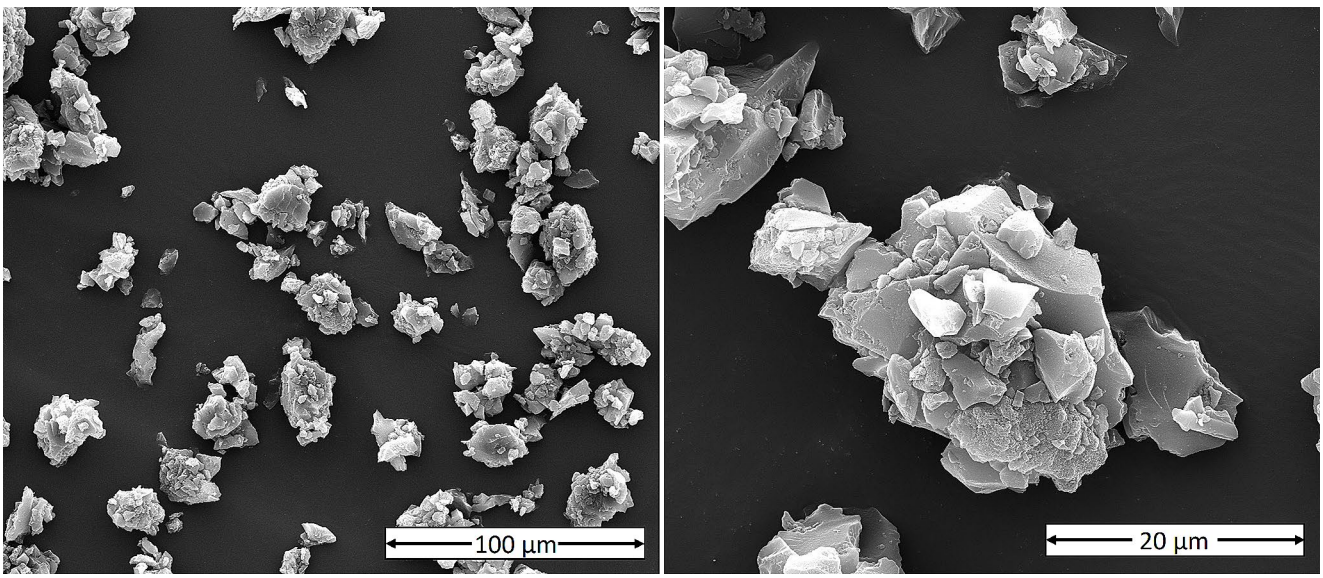

Fig. 1 SEM images at different magnifications of the BC particles used in this work

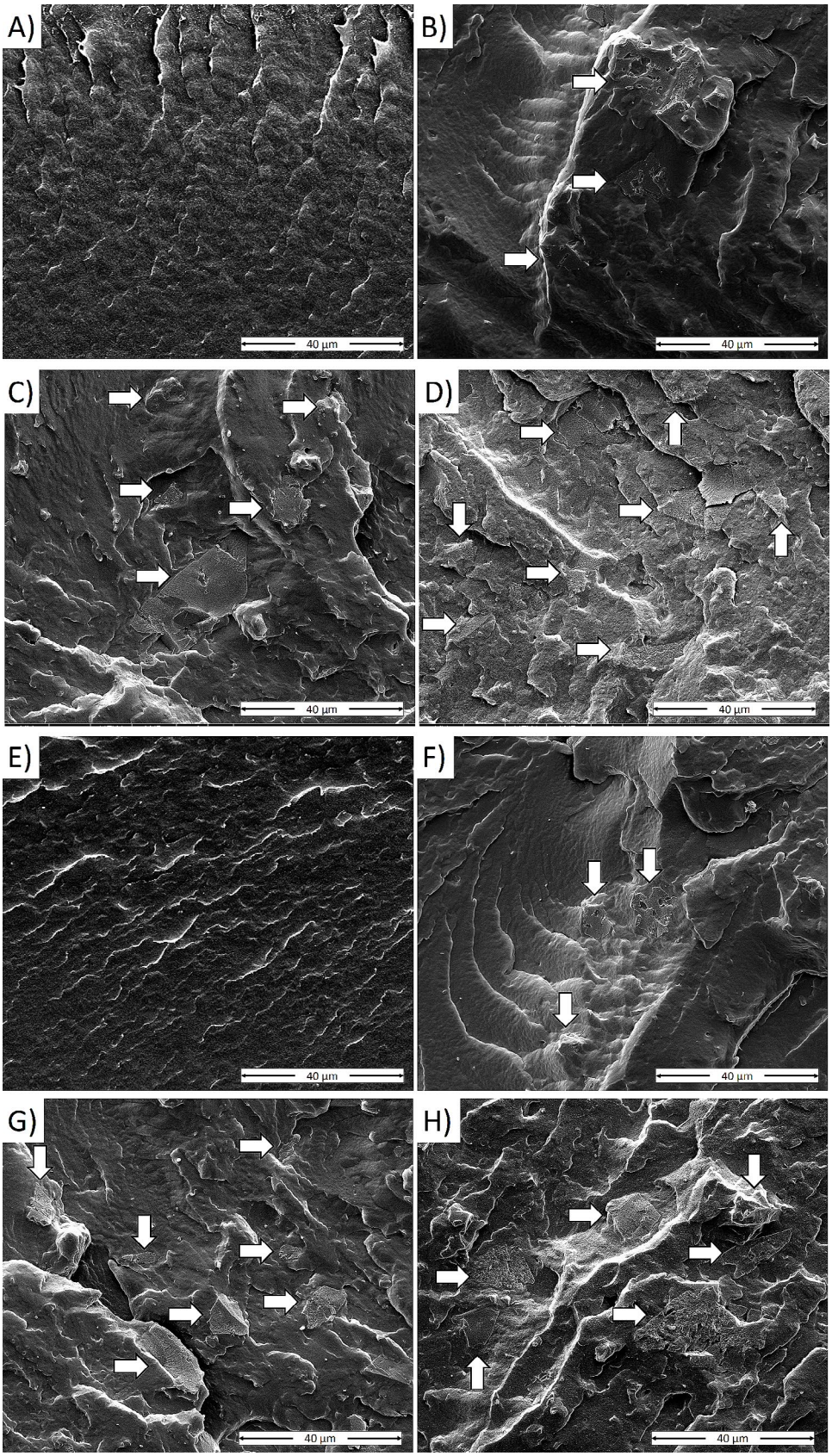

Fig. 2 SEM images at low magnification of the fractured surface of (**A**) PBAT, (**B**) PBAT/BC_5, (**C**) PBAT/BC_10, (**D**) PBAT/CV/BC_20, (**E**) PBAT/CV, (**F**) PBAT/CV/BC_5, (**G**) PBAT/CV/BC_10, and (H) PBAT/CV/BC_20 composites

More in detail, SEM images of PBAT and PBAT/CV blend samples appeared more homogeneous than the composites and, as expected, no presence of particles was detected. Furthermore, the absence of pores on the PBAT/CV surface can reasonably suggest the formation of a homogenous blend between PBAT and CV without evident demixing phenomenon.

The arrows in Fig. 2 indicate the bigger particles identified in the fractured surfaces although many smaller BC particles can be recognized in the micrographs of PBAT/BC and PBAT/CV/BC samples. As expected, the number of particles increased upon increasing the BC concentration, independently from the presence of CV in the composites. Furthermore, the size of the BC particles increased upon increasing the BC concentration in the composites, suggesting the formation of aggregates. Moreover, if compared to PBAT/BC composites (Fig. 2B-D), the ternary PBAT/CV/BC systems (Fig. 2F-H) showed BC particles with higher diameter, in particular at the highest concentrations (10 PHR and 20 PHR). This result suggests that the dispersion of the BC particles is more difficult when mixed with PBAT/CV blends, probably because of the lower viscosity of the samples containing CV, as will be discussed later.

The SEM images of the composites are shown in Fig. 3 at higher magnification to better observe the PBAT/BC interface. The inclusion of BC particles led to a final structure of the biocomposites in which the separation surface between particle and matrix is difficult to identify. Although qualitative, this result suggests a good polymer/filler affinity, also in the presence of CV in the composites, and it was confirmed by rheological and DSC analysis that will be discussed after.

Moreover, the porous structure of the BC appears partially filled by the polymer. This result can be ascribed to the high pressure set for the hot press processing likely able to fill the fillers' pores with the melt polymer matrix.

Rheological Characterization of PBAT-Based Composites

The effect of CV and BC concentration on the rheological properties of the PBAT-based biocomposites was analyzed by measuring the storage modulus (G'), the loss modulus (G''), and the complex viscosity (η*) as a function of frequency (Fig. 4). If compared with pure PBAT, PBAT/BC biocomposites showed a progressive increase in the values of G' (Fig. 4A), G'' (Fig. 4B), and complex viscosity (Fig. 4C) as the filler concentration increased. In scientific literature, a similar effect was already observed for polymeric composites filled with BC [35–37]. However, the

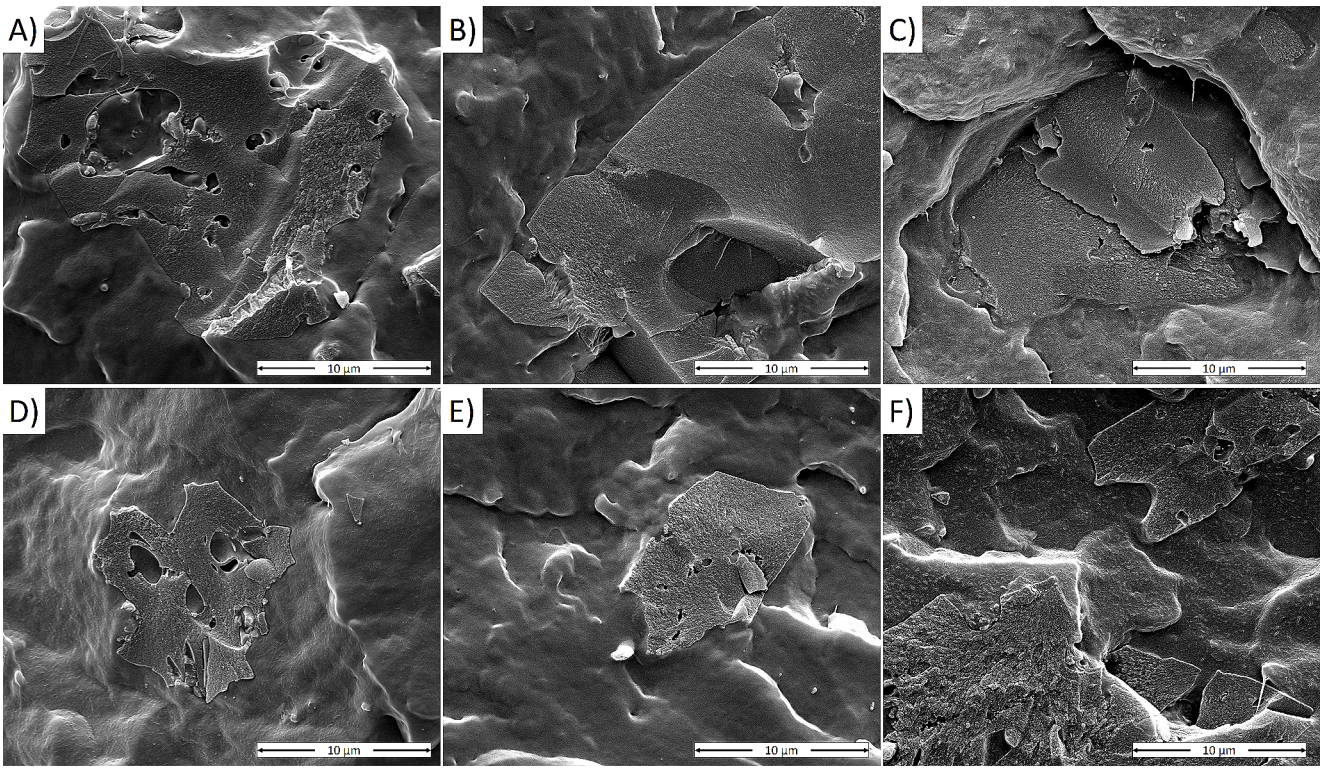

Fig. 3 SEM images at high magnification of the fractured surface of (**A**) PBAT/BC_5, (**B**) PBAT/BC_10, (**C**) PBAT/BC_20, (**D**) PBAT/CV/BC_5, (**E**) PBAT/CV/BC_10, and (**F**) PBAT/CV/BC_20 composites

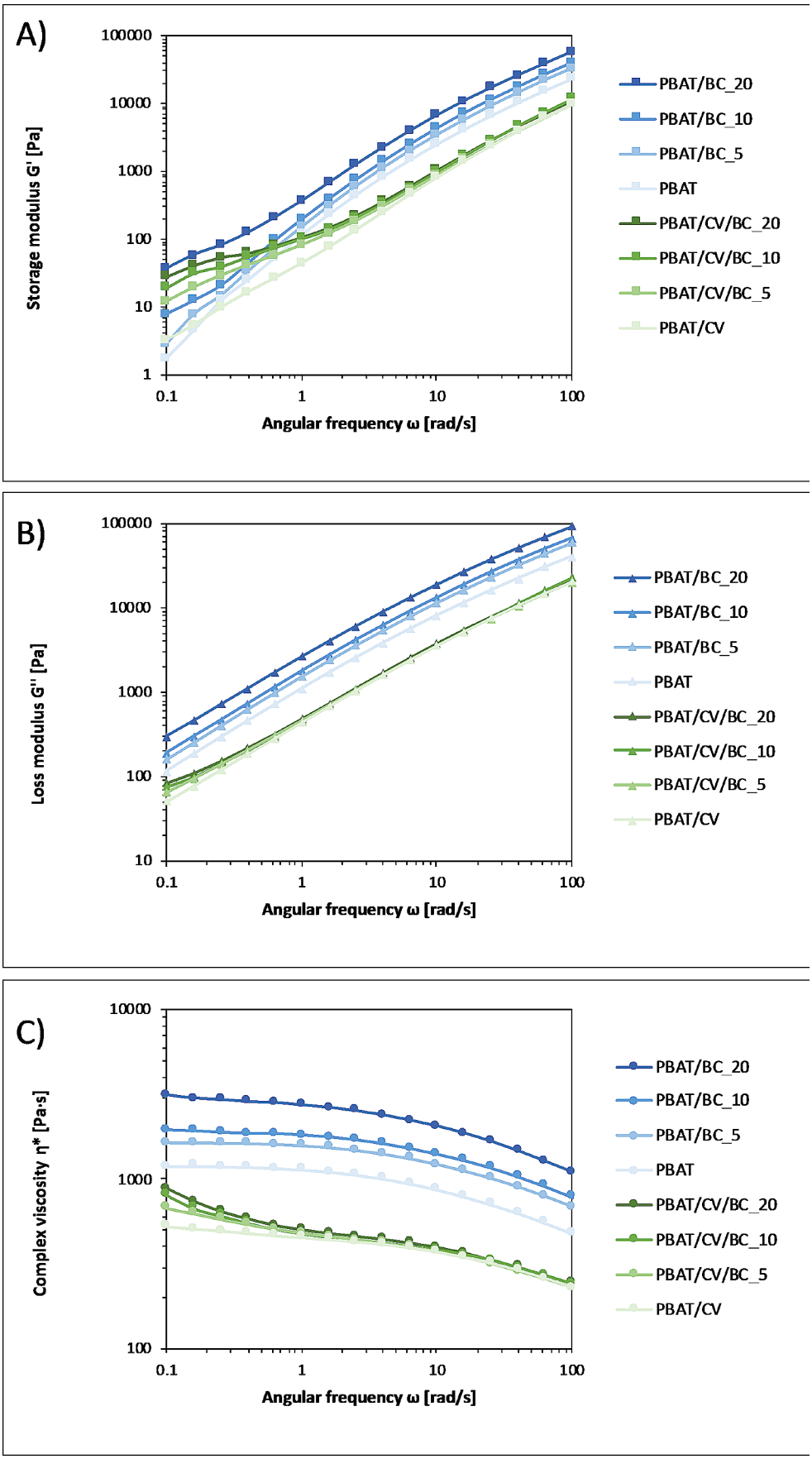

Fig. 4 (**A**) Storage modulus, (**B**) Loss modulus, and (**C**) Complex viscosity of melt PBAT-based composites

effect of the filler on the rheological behavior of the PBAT-based samples was different in the presence or not of CV in the mixture.

The addition of BC to PBAT induced an increase of G' for all the investigated frequencies although it was more noticeable at low frequencies. As a consequence, as the filler concentration increases, the slope of G' of PBAT/BC composites at low frequencies decreases, resulting in a more pronounced solid-like behavior, in particular for the PBAT/BC composites at the highest filler concentrations. This behavior can be ascribed to the formation of an interconnected network within the polymer matrix which limits the long-range movement of the polymer chains [38]. This result can be related to good particle dispersion and good compatibility with the polymer matrix [39]. In PBAT/BC samples, also G'' shows a similar trend since it increases as the BC concentration increases although the increase of G'' is lower than those of G'. Similar results have been highlighted by Pinheiro et al. [40] who attribute these findings to the increased particle dispersion, which improves the stress transfer between the matrix and the filler and consequently causes an increase of both G' and G''.

The addition of 20 PHR of CV in the systems (PBAT/CV and PBAT/CV/BC samples), caused a reduction of both G' and G'' moduli and the complex viscosity if compared to PBAT. This result can be probably ascribed to the low molecular weight of CV which may facilitate the macromolecular sliding and orientation under applied shear stress [41]. By observing the rheological behavior of the PBAT/CV/BC samples (and in particular those containing 20 PHR of BC), the presence of CV differently affects the value of G' at low and high frequencies. In fact, at high frequencies, the behavior of G' and of the complex viscosity of samples that contain CV are mainly governed by the PBAT/CV matrix behavior resulting in an overlapping of the curves regardless of the concentration of BC. On the other hand, the rheology of the same samples is governed by the filler at low frequencies due to the formation of an interconnected network, as already observed for the systems without CV.

As a result, by comparing the complex viscosity of PBAT/BC samples with that of PBAT/CV/BC samples from 0.1 rad/s to 1 rad/s it is possible to observe a transition from a pseudo-Newtonian behavior for PBAT/BC samples to a shear thinning behavior for PBAT/CV/BC, mostly visible at high BC concentrations [42].

Mechanical Properties

Tensile tests were performed to evaluate the effect of BC and CV on the mechanical behavior of PBAT. Fig. 5 shows the stress-strain curves obtained for biocomposites containing increasing amounts of BC (5, 10, and 20 PHR) in the absence or presence of CV (20 PHR). Figure 6A, B and C show elastic modulus (E), tensile strength (TS), and elongation at break (EB), respectively, as a function of the BC concentration.

Pure PBAT shows the mechanical behavior of a ductile polymer highlighting relatively low elastic modulus (~62 MPa), relatively high tensile strength (~27 MPa), and high ultimate strain (~1298%), values consistent with those found in the scientific literature [41–43]. The high tensile strength values can be ascribed to the ability of PBAT polymer chains to reorganize when subjected to high elongations thus undergoing to a stress-induced crystallization [44].

Graphs in Fig. 6 show that the elastic modulus of PBAT and PBAT/CV increased upon increasing the content of BC

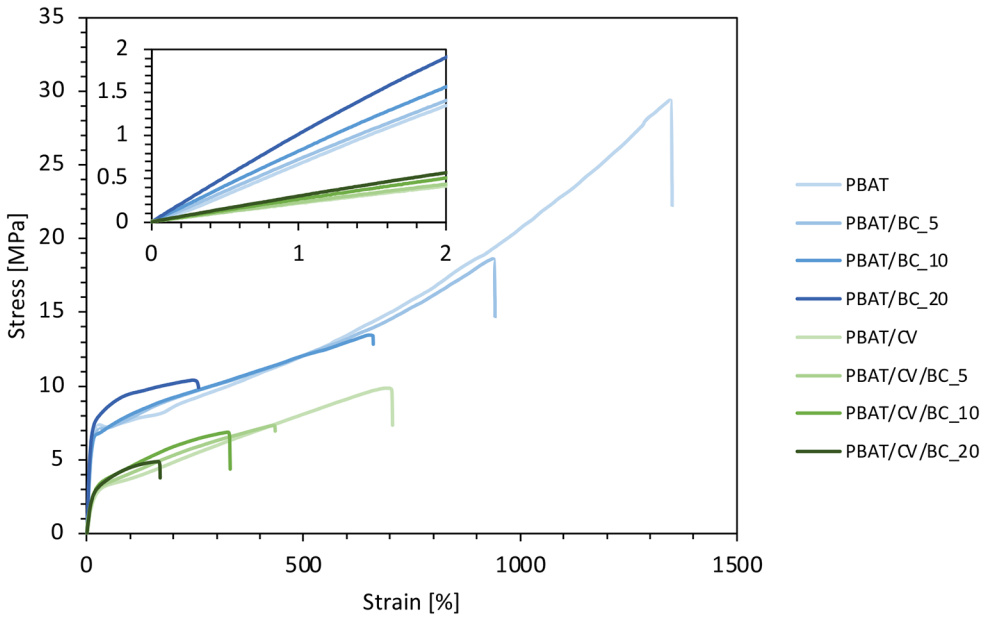

Fig. 5 Representative nominal stress-strain curves of PBAT-based biocomposites

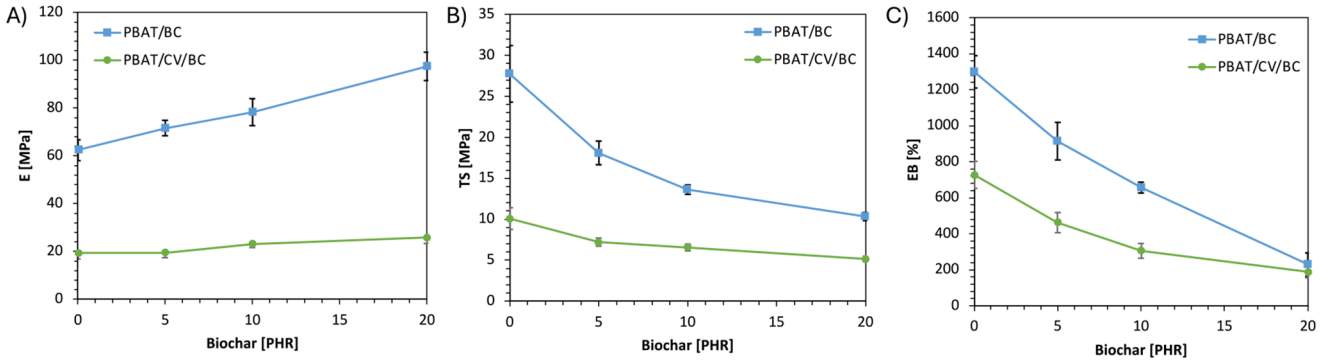

Fig. 6 (**A**) Elastic modulus, (**B**) tensile strength, and (**C**) elongation at break of PBAT and PBAT/CV films as a function of biochar PHR

while tensile strength and elongation at break decreased. The same Figure highlights that the presence of CV led to a decrease in all the mechanical properties investigated with respect to the polymer matrix.

The addition of BC particles (PBAT/BC samples) increased the elastic modulus of the polymer matrix by 15%, 25%, and 54% for biocomposites containing increasing percentages of BC up to 20 PHR demonstrating the reinforcing role of BC for PBAT. Those results agree with the scientific literature [36, 45–51] and can be ascribed to a reduction of the polymeric chain mobility due to the presence of solid particles. Furthermore, the BC particles can divert part of the stress from the polymer matrix, increasing the material stiffness [23].

On the other hand, as observed by SEM analysis, high BC concentration caused particle aggregation phenomena and cluster formation which may lead to an increase in stress concentration areas and a decrease in tensile strength (of about 32%, 46%, and 60%) ascribable to a reduction of the elongation at break (of about 32%, 48%, and 63% for BC PHR equal to 5, 10, and 20, respectively). The filler, therefore, was able to make the material more rigid and less ductile than pure PBAT but not brittle since the values of elongation at break remain above 200%, which is of interest for several applications including flexible food packaging.

The effect of the CV addition to the PBAT/BC samples decreased the reinforcing action of BC particles if compared to that observed on PBAT. In fact, the elastic moduli of PBAT/CV samples remain constant with the addition of 5 PHR of BC and then increase by 19% and 33% for PBAT/CV/BC_10 and PBAT/CV/BC_20, respectively. A decrease in tensile strength of 29%, 36%, and 48% and a decrease in elongation at break of 36%, 58% and 73% was found for PBAT/CV/BC_5, PBAT/CV/BC_10, and PBAT/CV/BC_20 samples, respectively, if compared to PBAT/CV.

The decrease in the elastic modulus can be related to the molecular interactions among PBAT molecules and CV which could facilitate the sliding of the polymer chains during deformation compromising the mechanical strength of the material, as already observed in several previous works [52–54] and coherently with the rheological analyses. This characteristic may also affect the ability of the BC particles to transfer the stress on the polymer matrix, resulting in the lower reinforcing action recorded with the tensile tests.

Regarding the reduction of tensile strength, an important factor may be the partial replacement of the strong interactions existing between the polymer chains with weak interactions between the polymer chain and CV molecules, according to the rheological measurements [41]. The presence of 20 PHR of CV caused a reduction of the elongation at break of the films except for those containing 20 PHR of BC where the elongation with and without CV was found to be comparable. A similar behavior was highlighted by the study conducted by Cardoso et al. [52] on PBAT films with increasing concentrations of oregano essential oil (OEO). The authors found that for high OEO concentrations (higher than 5 PHR), the additive is able to weaken the interactions between the polymer chains reducing the elongation of their PBAT-based films [52]. Other studies reported similar behaviors, including those carried out by Guo et al. about soy protein isolate (SPI) and PBAT films [55] and Lopez-Mata et al. [56] about chitosan films incorporated with CV.

For flexible food packaging applications, the TS of polymeric materials should be greater than 3.5 MPa [41]. The results obtained for all the samples show higher values, adequate values of tensile strength, and high values of elongation at break and therefore make them suitable for such applications.

Thermal Properties of the PBAT-Based Films

Fig. 7A and B show the cooling and heating curves obtained by DSC of the biocomposites. Table 2 shows the crystallization temperature (T_c), melting temperature (T_m), enthalpy of crystallization (ΔH_c), melting enthalpy, and crystallinity (X_c).

Pure PBAT shows a T_c of 72 °C, a T_m of 122 °C, and a crystallinity of 11.7%. By adding BC particles, an increase

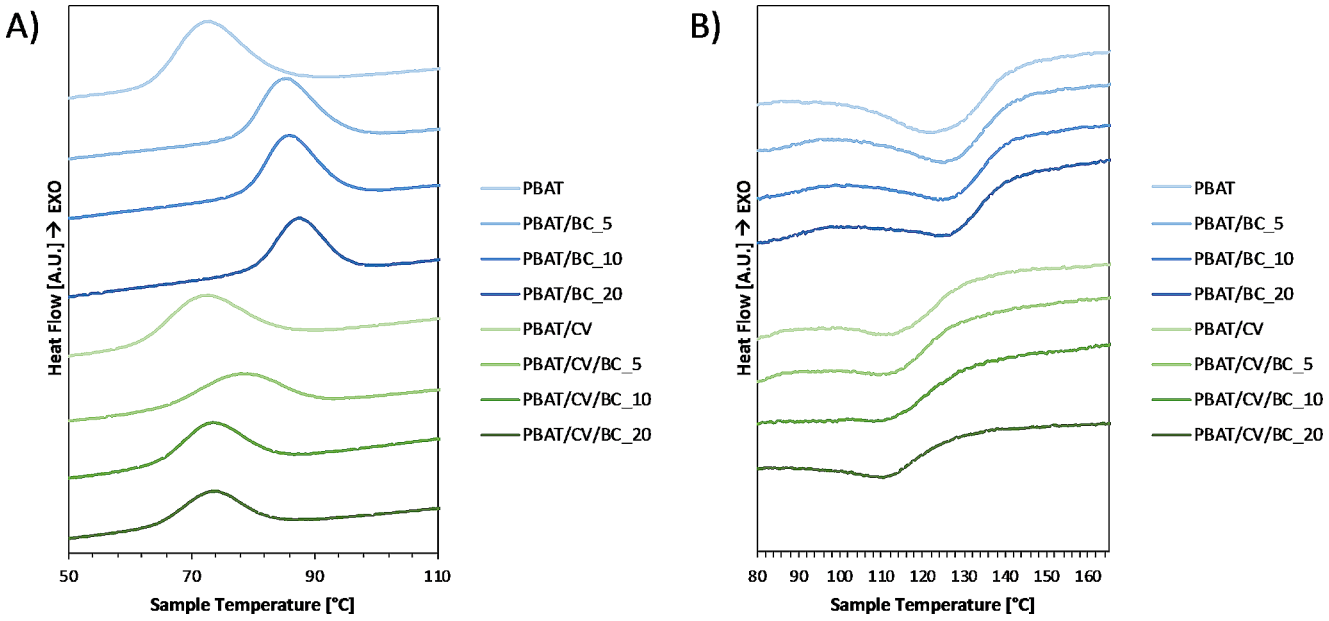

Fig. 7 DSC (**A**) cooling and (**B**) second heating thermograms of PBAT-based films

Table 2 Thermal properties of PBAT-based films

Sample	Cooling		II Heating		
	T_c [°C]	ΔH_c [j/g]	T_m [°C]	ΔH_m [j/g]	X_c [%]
PBAT	72.19 ± 2.17	20.95 ± 0.59	122.51 ± 0.91	13.34 ± 0.13	11.7 ± 0.13
PBAT/BC_5	85.22 ± 2.39	15.56 ± 0.54	125.34 ± 1.19	10.1 ± 0.11	9.31 ± 0.14
PBAT/BC_10	85.88 ± 3.01	15 ± 0.65	126.33 ± 1.37	8.46 ± 0.13	8.16 ± 0.16
PBAT/BC_20	87.6 ± 2.77	11.81 ± 0.67	126.78 ± 1.92	7.82 ± 0.15	8.23 ± 0.15
PBAT/CV	71.86 ± 2.1	14.96 ± 0.64	112.55 ± 2.17	6.02 ± 0.04	6.33 ± 0.05
PBAT/CV/BC_5	77.91 ± 2.35	11.6 ± 0.37	113.34 ± 1.72	6.02 ± 0.11	6.61 ± 0.12
PBAT/CV/BC_10	73.47 ± 2.35	11.58 ± 0.63	110.46 ± 1.95	6.7 ± 0.12	7.64 ± 0.14
PBAT/CV/BC_20	73.3 ± 2.96	10.02 ± 0.33	110.45 ± 1.95	6.11 ± 0.2	7.51 ± 0.17

of up to 15 °C in T_c was observed while a very slight increase of T_m (up to 4 °C) and a very slight slight decrease (down to 3%) in crystallinity was detected. The significant increase in crystallization temperature can be ascribed to the nucleating effect of the BC particles. In fact, particles having aromatic chemical structures are able to act as a nucleating agent for semi-crystalline polymers containing an aromatic ring in their backbones through π-π interactions [57]. Therefore, the crystallization of the butylene terephthalate (BT) units of PBAT can be favored by the aromatic structure of the particle.

However, a decrease in ΔH_c and ΔH_m was observed as the BC content increased as well as a very slight reduction in crystallinity. This result can be likely explained by assuming that BC particles are able to accelerate the crystallization of PBAT while they inhibit the growth of crystallites by hindering the rearrangement of the PBAT molecular chains during the crystallization process [58], thus leading to an incomplete crystallization during cooling [57].

Finally, the increase in T_m can be related to the promotion of crystallization kinetics allowing the formation of a more ordered crystalline structure characterized by smaller and more perfect grains that melt at a higher temperature [17, 57, 58], although other investigations will be carried out to support this hypothesis.

The addition of CV (PBAT/CV samples) does not change the T_c value, while it slightly increases upon increasing the BC concentration (PBAT/CV/BC samples). The same behavior was found by da Costa et al. [59] on PHBV film with essential oil of oregano and clay nanoparticles. However, the addition of CV led to a decrease in T_m also in the presence of the filler. Similarly, there is a reduction in the crystallinity of the films probably due to the increased mobility of the polymer chain due to CV. Similar results were already observed in previous works of da Costa et al. [59], Cui et al. [60] Liu et al. [61] and Silva et al. [62]. If compared to PBAT/CV samples, a very slight increase in crystallinity is then observed in PBAT/CV/BC samples as the amount of BC increases. This can be explained by considering the

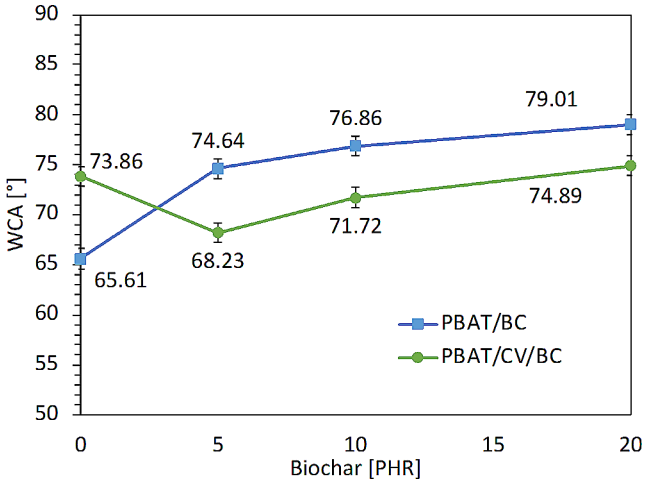

Fig. 8 WCA measurements of PBAT and PBAT/CV films as a function of the biochar PHR

combination of two factors: the increased mobility of the polymer chains promoted by CV and the nucleating effect of the BC particles, as mentioned previously.

Wettability of the PBAT-Based Films

Water contact angle (WCA) is essential for investigating the wettability of biopolymeric films, and therefore the hydrophilic or hydrophobic character of their surface. Fig. 8 shows the trend of the contact angle as a function of the percentage of BC added to PBAT and PBAT/CV samples.

Generally, a polymeric film can be defined as hydrophobic if its WCA is greater than 65° [63–65], while lower WCA values are obtained by hydrophilic materials. WCA data revealed that all the films are characterized by a hydrophobic behavior, especially as the filler content increases. These results are of considerable interest as regards a possible application of the materials obtained in the packaging sector since a low hydrophilicity in the materials is desired [30]. More in detail, pure PBAT has an average WCA value of about 66°, a value in agreement with the results found in the scientific literature [63], which gives the film a slightly hydrophobic character despite the presence of polar groups [64]. The addition of CV (PBAT/CV samples) led to a slight increase of the WCA that raised at ~74°. This result can be explained considering the hydrophobic characteristic of CV [66–68] which could affect the chemical surface properties of the PBAT/CV blends as will be discussed after.

The WCA values of the CV-containing composite films (PBAT/CV/BC samples) are slightly lower, however the hydrophobic character of the materials is still maintained.

Increasing BC content made the PBAT/CV/BC samples increasingly hydrophobic and this is mainly ascribable to the hydrophobic nature of the particles. In fact, the hydrophobicity of BC is strongly dependent on the pyrolysis temperature used for the manufacturing process, i.e. the higher the processing temperature the higher the loss of hydroxyl groups of the lignocellulosic backbone, leading to more hydrophobic particles [50].

In order to better understand the effect of CV on the chemical properties of PBAT surface, FTIR-ATR analysis was carried out and reported in Figs. 9, 10. The typical FTIR peaks related to PBAT are clearly visible, including -OH vibrations at ca. 3400–3450 cm^{-1}, whereas bands at 2957 cm^{-1} and 2874 cm^{-1} can be assigned to a CH_2 stretching mode. The carbonyl groups (C=O) presented a strong peak around 1710 cm^{-1}, with a sharp peak representing CH_2

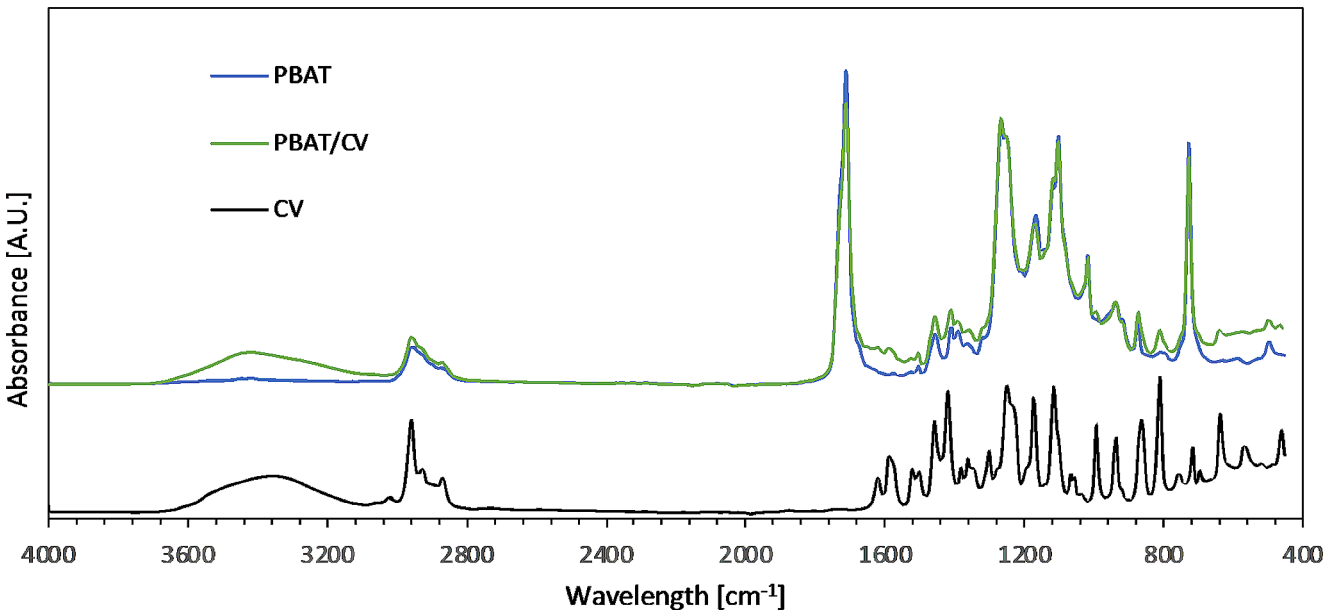

Fig. 9 FTIR-ATR spectra of PBAT, Carvacrol, and PBAT/CV blend

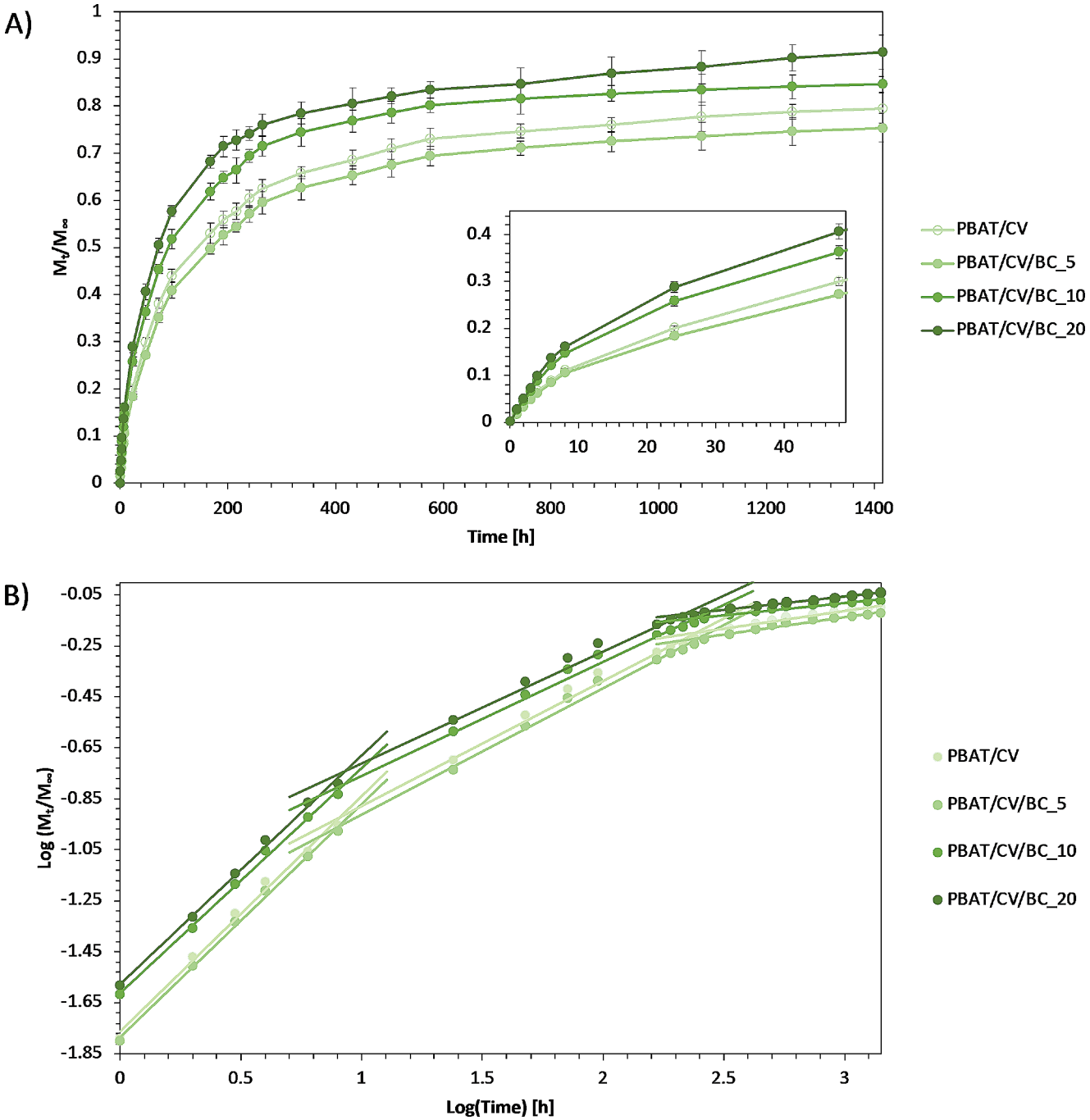

Fig. 10 Release kinetics of CV from PBAT-based films in distilled water at 4 °C expressed as (**A**) M_t/M_∞ vs. Time and (**B**) Log(M_t/M_∞) vs. Log(Time)

groups at 720 cm^{-1}. The C–O bond in the ester linkage was observed at around 1275–1250 cm^{-1} [24].

CV shows characteristic peaks at 3378 cm^{-1} (-OH), 2960 cm^{-1} (CH stretching), 1459 cm^{-1}, 1382 cm^{-1} and 1346 cm^{-1} (CH deformation), and 866 cm^{-1} and 812 cm^{-1} (aromatic ring) [29]. FTIR-ATR of PBAT/CV blends showed that several CV bands were overlapped by the more intense PBAT peaks. Nevertheless, the broad peak related to -OH vibrations at ca. 3200–3450 cm^{-1} in PBAT/CV is much more intense than in PBAT samples [69, 70]Other peaks of PBAT/CV spectrum that can be related to CV molecules are the CH stretching at 2960 cm^{-1}, the CH deformation at 1459 cm^{-1} and, more evidently, the hydrophobic benzene ring at 812 cm^{-1} [71], demonstrating the effective mixing of PBAT and CV.

It is well known that oxygenated moieties on polymeric surfaces are able to decrease the WCA of samples by increasing the cohesive forces with water [69, 70]. However, the increase of the WCA of PBAT when blended with CV (PBAT/CV samples) suggests that the resulting hydrophobic character of the film is mainly governed by the hydrophobic benzene ring of CV present on the surface of the PBAT/CV films.

Carvacrol Release Kinetic

Fig. 9A shows the cumulative release of CV expressed as the ratio between the amount released at a given time t (M_t) and the theoretical amount of CV incorporated in the samples (M_∞), equal to the absolute amount of drug incorporated within the system, as a function of time. For all the systems, the CV release was characterized by three phases: (i) a burst phase in the first 8 h of release; (ii) a second phase characterized by a slower release rate; and (iii) a release plateau after 312 h.

The BC content affected the amount of CV released if compared to PBAT/CV samples. In fact, PBAT/CV/BC_5 samples presented the lowest final value of M_t/M_∞, however, a higher value of this ratio was observed as the amount of BC increased, respectively for the 10 PHR and 20 PHR systems. During the first 8 h the fractions released by the PBAT/CV, PBAT/CV/BC_5, PBAT/CV/BC_10, and PBAT/CV/BC_20 samples are respectively 11%, 10%, 15%, and 16%. After 48 h the fractions rise to 20%, 18%, 26%, and 29%. At the end of the test, after 1416 h, values equal to 79%, 75%, 85% and 91% are reached. It is therefore possible to deduce that low quantities of filler hinder the diffusion of CV molecules due to the tortuous path they create, high quantities have an opposite effect, leading to the creation of preferential paths that ease the CV diffusion out of the polymer matrix. This result is also coherent with SEM analysis that highlighted the presence of BC aggregates in particular at high filler concentrations for PBAT/CV/BC samples.

To study the diffusion mechanism and kinetics, the experimental data (reported in Fig. 9B by plotting the Log (M_t/M_∞) versus Log (time) were fitted using the following power law model [8] (Eq. 2):

$$\frac{M_t}{M_\infty} = kt^n \tag{2}$$

Where t is the release time, k is a kinetic constant related to the rate of release of the substance and n is the diffusion exponent which indicates the mechanism of release. If n is lower than 0.5 the release is governed by diffusion phenomena (Fickian); if n is 1 the release is governed by swelling phenomena, if n is between 0.5 and 1.0, an anomalous diffusion occurs due to a combination of diffusion and swelling phenomena [30]. Table 3 summarizes the values of the power law parameters obtained from the release kinetics of CV.

The analysis of the parameter n indicates that, in the first stage, the release mechanisms of all the samples are characterized by an anomalous transport although mainly controlled by swelling phenomena since all the values are around 0.9. In the second and third stages, Fickian diffusion release mechanism was detected. The release kinetics is confirmed by the analysis of k, in fact, the systems loaded at 10 PHR and 20 PHR of BC are those with the fastest release in all three stages.

Although it is often regarded as an instability problem, the burst release of active compounds can enhance their antimicrobial effectiveness by increasing their availability during the first hours of contact with the target surface [72]. Then, the sustained release of the antimicrobial compounds allows for prolonged antibacterial effects.

Antibacterial Properties of PBAT-Based Films

The results of the antibacterial properties of the biocomposite PBAT/CV/BC films against the main four pathogenic bacteria (*E. coli*; *L. monocytogenes*; *S.* Enteritidis and *St. aureus*), responsible for food-borne diseases outbreaks [73], are reported in Table 4. At the beginning of monitoring (0 d), all pathogenic bacteria showed levels almost the same as those for inoculation, confirming that inoculums occurred at 10^6 CFU/mL. Significant differences ($p < 0.0001$) were found from the 2nd sampling time (1 d) for the levels of all strains object of investigation among the different biocomposite PBAT films. In particular, except for the PBAT and PBAT/BC_20 samples produced without the addition of CV, all other materials containing CV regardless of the percentage of BC added, determined a decrease of the four pathogenic bacteria below the detection limit (< 1 Log CFU/mL).

These observations are not surprising because the inability of PBAT film to inhibit the growth of pathogenic bacteria

Table 3 Power law parameters obtained from the release kinetics of CV

	I Stage			II Stage			III Stage		
Sample	k [h^{-1}]	n	R^2	k [h^{-1}]	n	R^2	k [h^{-1}]	n	R^2
PBAT/CV	0.172	0.922	0.993	0.254	0.491	0.989	0.588	0.139	0.970
PBAT/CV/BC_5	0.168	0.915	0.997	0.245	0.496	0.993	0.579	0.137	0.966
PBAT/CV/BC_10	0.200	0.883	0.997	0.299	0.448	0.990	0.691	0.096	0.953
PBAT/CV/BC_20	0.207	0.896	0.996	0.316	0.440	0.984	0.687	0.106	0.995

Table 4 Antimicrobial activity of PBAT-based films against the main food-borne bacterial pathogens

Strains/Samples	Day		
	0	1	3
E. coli ATCC25922			
PBAT	6.18 ± 0.11 a	6.09 ± 0.12 a	6.06 ± 0.18 a
PBAT/BC_20	6.05 ± 0.17 a	5.14 ± 0.15 b	5.09 ± 0.12 b
PBAT/CV	6.04 ± 0.16 a	< 1 c	< 1 c
PBAT/CV/BC_5	5.95 ± 0.19 a	< 1 c	< 1 c
PBAT/CV/BC_10	6.09 ± 0.13 a	< 1 c	< 1 c
PBAT/CV/BC_20	6.06 ± 0.10 a	< 1 c	< 1 c
p-value	0.586	< 0.0001	< 0.0001
L. monocytogenes ATCC19114			
PBAT	6.13 ± 0.16 a	6.06 ± 0.21 a	6.04 ± 0.16 a
PBAT/BC_20	6.16 ± 0.20 a	5.70 ± 0.14 b	5.45 ± 0.21 b
PBAT/CV	6.15 ± 0.17 a	< 1 c	< 1 c
PBAT/CV/BC_5	6.16 ± 0.11 a	< 1 c	< 1 c
PBAT/CV/BC_10	6.12 ± 0.18 a	< 1 c	< 1 c
PBAT/CV/BC_20	5.94 ± 0.13 a	< 1 c	< 1 c
p-value	0.552	< 0.0001	< 0.0001
S. Enteritidis ATCC13076			
PBAT	6.09 ± 0.13 a	6.03 ± 0.14 a	6.03 ± 0.14 a
PBAT/BC_20	6.10 ± 0.13 a	5.27 ± 0.13 b	5.25 ± 0.10 b
PBAT/CV	6.24 ± 0.20 a	< 1 c	< 1 c
PBAT/CV/BC_5	6.03 ± 0.14 a	< 1 c	< 1 c
PBAT/CV/BC_10	6.23 ± 0.15 a	< 1 c	< 1 c
PBAT/CV/BC_20	5.97 ± 0.10 a	< 1 c	< 1 c
p-value	0.220	< 0.0001	< 0.0001
St. aureus ATCC33862			
PBAT	6.14 ± 0.15 a	6.07 ± 0.10 a	6.06 ± 0.13 a
PBAT/BC_20	6.20 ± 0.14 a	5.90 ± 0.14 b	5.85 ± 0.11 b
PBAT/CV	5.90 ± 0.14 a	< 1 c	< 1 c
PBAT/CV/BC_5	6.12 ± 0.15 a	< 1 c	< 1 c
PBAT/CV/BC_10	6.17 ± 0.13 a	< 1 c	< 1 c
PBAT/CV/BC_20	6.18 ± 0.17 a	< 1 c	< 1 c
p-value	0.210	< 0.0001	< 0.0001

such as *E. coli* and *St. aureus* was previously reported by Venkatesan & Rajeswari [74]. Therefore, the resulting inhibition activity of these materials is due to the presence of CV rather than BC. In fact, it is well known that this phenolic monoterpene is able to inhibit the growth of Gram-positive and Gram-negative undesired pathogenic bacteria when it is included in polymeric matrices [5, 7, 75]. In particular, the inhibition activity of these materials is explained for Gram-positive bacteria by the ability of CV to move through the peptidoglycan layer and then act on the cytoplasmic membrane [76], while for the Gram-negative bacteria to spread and destroy their external lipopolysaccharide covering [77, 78].

Units are Log CFU/mL. Results indicate the mean values ± standard deviation (S.D.) of two plate counts. Data within a column followed by the same letter are not significantly different according to Tukey's test. Abbreviations: *E.*, *Escherichia*; *L.*, *Listeria*; *S.*, *Salmonella*; *St.*, *Staphylococcus*; PBAT, Polybutylene adipate terephthalate; CV, carvacrol; BC, biochar.

Conclusions

In this work, the chemo-physical characterization and antimicrobial potential of PBAT-based biocomposite films loaded with 20 PHR of CV and different amounts of BC (5, 10, and 20 PHR) were evaluated and compared to PBAT/BC films. The results revealed that the addition 20 PHR of CV to PBAT/BC composites strongly modify their chemical physical properties. In fact, rheological measurements showed an overall decrease in the complex viscosity of the samples, thus highlighting the sliding efficacy of CV for the PBAT molecules. The mechanical properties revealed that

the ternary PBAT/CV/BC samples still maintain values of elastic modulus, tensile strength, and elongation at break suitable for applications in flexible active food packaging. WCA analysis underlined that the hydrophobic character of the materials is still maintained. The BC content affected the amount of CV released if compared to PBAT/CV samples although it was not able to strongly reduce the burst release of CV. In fact, low quantities of BC hinder the diffusion of CV molecules due to the tortuous path they generate, while high quantities have the opposite effect, leading to the creation of preferential paths that ease the CV diffusion out of the polymer matrix. From the microbiological point of view, all PBAT films containing CV regardless of the percentage of BC added, showed the ability to inhibit all four pathogenic bacteria below the detection limit. In the future, in vivo tests with food matrices will be carried out to assess the antimicrobial efficacy of the PBAT/CV/BC films as flexible food packaging.

Author Contributions F.L., L.B., G.P., and G.G.: Investigation; F.L., L.B., G.G., and R.G.: Data curation; F.L., L.B., and R.G.: Writing—original draft preparation; F.L.: Writing – review & editing; L.B.: Conceptualization; L.B. and R.G.: Supervision.

Funding F.L. is partially supported by European Social Fund (ESF) - Complementary Operational Programme (POC) 2014/2020 of the Sicily Region.
Open access funding provided by Università degli Studi di Palermo within the CRUI-CARE Agreement.

Data Availability No datasets were generated or analysed during the current study.

Declarations

Conflict of interest The authors declare that they have no known competing financial interests or personal relationships that could have appeared to influence the work reported in this paper.

References

1. Luo H, Yin X-Q, Tan P-F et al (2021) Polymeric antibacterial materials: design, platforms and applications. J Mater Chem B 9:2802–2815. https://doi.org/10.1039/D1TB00109D
2. Qiu H, Si Z, Luo Y et al (2020) The mechanisms and the applications of antibacterial polymers in surface modification on medical devices. Front Bioeng Biotechnol 8:910
3. Ding X, Wang A, Tong W, Xu F-J (2019) Biodegradable antibacterial polymeric nanosystems: a new hope to cope with multidrug-resistant bacteria. Small 15:1900999
4. Scaffaro R, Lopresti F, Marino A, Nostro A (2018) Antimicrobial additives for poly(lactic acid) materials and their applications: current state and perspectives. Appl Microbiol Biotechnol 102:1–18. https://doi.org/10.1007/s00253-018-9220-1
5. de Souza AG, Dos Santos NMA, da Silva Torin RF, dos Santos Rosa D (2020) Synergic antimicrobial properties of Carvacrol essential oil and montmorillonite in biodegradable starch films. Int J Biol Macromol 164:1737–1747. https://doi.org/10.1016/j.ijbiomac.2020.07.226
6. Xiao L, Yao Z, He Y et al (2022) Antioxidant and antibacterial PBAT/lignin-ZnO nanocomposite films for active food packaging. Ind Crops Prod 187:115515
7. Gaglio R, Botta L, Garofalo G et al (2021) Carvacrol activated biopolymeric foam: an effective packaging system to control the development of spoilage and pathogenic bacteria on sliced pumpkin and melon. Food Packag Shelf Life 28:100633. https://doi.org/10.1016/j.fpsl.2021.100633
8. Lopresti F, Botta L, La Carrubba V et al (2022) Physical and antibacterial properties of PLA Electrospun mats loaded with carvacrol and nisin. Express Polym Lett 16:1083–1098. https://doi.org/10.3144/expresspolymlett.2022.79
9. Qiu S, Zhou Y, Waterhouse GIN et al (2021) Optimizing interfacial adhesion in PBAT/PLA nanocomposite for biodegradable packaging films. Food Chem 334:127487
10. Jian J, Xiangbin Z, Xianbo H (2020) An overview on synthesis, properties and applications of poly (butylene-adipate-co-terephthalate)-PBAT. Adv Industrial Eng Polym Res 3:19–26
11. Zhou S, Zhai X, Zhang R et al (2021) High-throughput fabrication of antibacterial starch/PBAT/AgNPs@ SiO2 films for food packaging. Nanomaterials 11:3062
12. Xu J, Lei Z, Liu S et al (2022) Preparation and characterization of biodegradable electrospinning PHBV/PBAT/TiO2 antibacterial nanofiber membranes. J Eng Fiber Fabr 17:15589250221136566
13. Xu Y, Huang C, Dang X et al (2020) Preparation of long-term antibacterial SiO2-cinnamaldehyde microcapsule via sol-gel approach as a functional additive for PBAT film. Processes 8:897
14. Laorenza Y, Harnkarnsujarit N (2021) Carvacrol, citral and α-terpineol essential oil incorporated biodegradable films for functional active packaging of Pacific white shrimp. Food Chem 363:130252
15. Łopusiewicz Ł, Macieja S, Bartkowiak A, El Fray M (2021) Antimicrobial, Antibiofilm, and antioxidant activity of functional poly (Butylene Succinate) films modified with curcumin and Carvacrol. Materials 14:7882
16. de Medeiros JAS, Blick AP, Galindo MV et al (2019) Incorporation of oregano essential oil microcapsules in starch-poly (butylene adipate co-terephthalate)(PBAT) films. In: Macromolecular Symposia. p 1800052
17. Fukushima K, Wu M-H, Bocchini S et al (2012) PBAT based nanocomposites for medical and industrial applications. Mater Sci Engineering: C 32:1331–1351. https://doi.org/10.1016/j.msec.2012.04.005

18. Li W, Huang J, Liu W et al (2022) Lignin modified PBAT composites with enhanced strength based on interfacial dynamic bonds. J Appl Polym Sci 139:e52476
19. Zhong B, Tang Y, Chen Y et al (2023) Improvement of UV aging resistance of PBAT composites with silica-immobilized UV absorber prepared by a facile method. Polym Degrad Stab 110337
20. Sun C, Li C, Li H et al (2022) Modified cellulose nanocrystals enhanced the compatibility between PLA and PBAT to prepare a multifunctional composite film. J Polym Environ 30:3139–3149
21. Bartoli M, Arrigo R, Malucelli G et al (2022) Recent advances in Biochar Polymer composites. Polym (Basel) 14. https://doi.org/10.3390/polym14122506
22. Kane S, Van Roijen E, Ryan C, Miller S (2022) Reducing the environmental impacts of plastics while increasing strength: Biochar fillers in biodegradable, recycled, and fossil-fuel derived plastics. Compos Part C: Open Access 8:100253. https://doi.org/10.1016/j.jcomc.2022.100253
23. George J, Jung D, Bhattacharyya D (2023) Improvement of Electrical and Mechanical properties of PLA/PBAT composites using Coconut Shell Biochar for Antistatic Applications. Appl Sci 13:902
24. Botta L, Teresi R, Titone V et al (2021) Use of Biochar as Filler for Biocomposite Blown films: structure-Processing-Properties relationships. Polym (Basel) 13:3953
25. Oun AA, Bae AY, Shin GH et al (2022) Comparative study of oregano essential oil encapsulated in halloysite nanotubes and diatomaceous earth as antimicrobial and antioxidant composites. Appl Clay Sci 224:106522
26. Sani IK, Pirsa S, Ta\ug\i \cSeref (2019) Preparation of chitosan/zinc oxide/Melissa officinalis essential oil nano-composite film and evaluation of physical, mechanical and antimicrobial properties by response surface method. Polym Test 79:106004
27. Scaffaro R, Maio A, Lopresti F (2019) Effect of graphene and fabrication technique on the release kinetics of carvacrol from polylactic acid. Compos Sci Technol 169:60–69. https://doi.org/10.1016/j.compscitech.2018.11.003
28. Scaffaro R, Botta L, Maio A, Gallo G (2017) PLA graphene nanoplatelets nanocomposites: physical properties and release kinetics of an antimicrobial agent. Compos B Eng 109:138–146. https://doi.org/10.1016/j.compositesb.2016.10.058
29. Lopresti F, Botta L, Scaffaro R et al (2019) Antibacterial biopolymeric foams: structure–property relationship and carvacrol release kinetics. Eur Polym J 121:109298. https://doi.org/10.1016/j.eurpolymj.2019.109298
30. Lopresti F, Botta L, La Carrubba V et al (2021) Combining carvacrol and nisin in biodegradable films for antibacterial packaging applications. Int J Biol Macromol 193:117–126. https://doi.org/10.1016/j.ijbiomac.2021.10.118
31. Dons\`\i F, Annunziata M, Vincensi M, Ferrari G (2012) Design of nanoemulsion-based delivery systems of natural antimicrobials: effect of the emulsifier. J Biotechnol 159:342–350
32. Gill AO, Holley RA (2006) Disruption of Escherichia coli, Listeria monocytogenes and Lactobacillus sakei cellular membranes by plant oil aromatics. Int J Food Microbiol 108:1–9
33. Seoane IT, Cortez Tornello PR, Silva L et al (2020) Development and validation of a mechanistic model for the release of embelin from a polycaprolactone matrix. Polym Test 91:106855. https://doi.org/10.1016/j.polymertesting.2020.106855
34. Jayabalakrishnan D, Prabhu P, Iqbal MS et al (2021) Mechanical, dielectric, and hydrophobicity behavior of coconut shell biochar toughened Caryota urens natural fiber reinforced epoxy composite. Polym Compos 43:493–502
35. Poulose AM, Elnour AY, Anis A et al (2018) Date palm biochar-polymer composites: an investigation of electrical, mechanical, thermal and rheological characteristics. Sci Total Environ 619–620:311–318. https://doi.org/10.1016/j.scitotenv.2017.11.076
36. Infurna G, Botta L, Ingargiola I et al (2023) Biochar from Digestate Pyrolysis as a Filler for Biopolymer blends: Effect of Blend Composition. J Polym Environ. https://doi.org/10.1007/s10924-023-03108-1
37. Wang Y, Liu X, Shi Z et al (2021) Rheological behavior of high density polyethylene (HDPE) filled with Corn Stalk Biochar. ChemistrySelect 6:10418–10428. https://doi.org/10.1002/slct.202102663
38. El Achaby M, Ennajih H, Arrakhiz FZ et al (2013) Modification of montmorillonite by novel geminal benzimidazolium surfactant and its use for the preparation of polymer organoclay nanocomposites. Compos B Eng 51:310–317
39. Adrar S, Habi A, Ajji A, Grohens Y (2017) Combined effect of epoxy functionalized graphene and organomontmorillonites on the morphology, rheological and thermal properties of poly (butylenes adipate-co-terephtalate) with or without a compatibilizer. Appl Clay Sci 146:306–315
40. Pinheiro IF, Ferreira FV, Alves GF et al (2019) Biodegradable PBAT-based nanocomposites reinforced with functionalized cellulose nanocrystals from Pseudobombax munguba: rheological, thermal, mechanical and biodegradability properties. J Polym Environ 27:757–766
41. de Andrade MF, de Lima Silva ID, da Silva GA et al (2020) A study of poly (butylene adipate-co-terephthalate)/orange essential oil films for application in active antimicrobial packaging. LWT 125:109148
42. Di Bella G, Corsino SF, De Marines F et al (2022) Occurrence of Microplastics in Waste Sludge of Wastewater treatment plants: comparison between membrane bioreactor (MBR) and Conventional activated Sludge (CAS) technologies. Membr (Basel) 12. https://doi.org/10.3390/membranes12040371
43. Moustafa H, Guizani C, Dufresne A (2017) Sustainable biodegradable coffee grounds filler and its effect on the hydrophobicity, mechanical and thermal properties of biodegradable PBAT composites. J Appl Polym Sci 134
44. Zhou J, Zheng Y, Shan G et al (2020) Stretch-induced crystalline structural evolution and cavitation of poly (butylene adipate-ran-butylene terephthalate)/poly (lactic acid) immiscible blends. Polym (Guildf) 188:122121
45. Zhang Q, Cai H, Yi W et al (2020) Biocomposites from organic solid wastes derived biochars: a review. Materials 13:3923
46. Haeldermans T, Samyn P, Cardinaels R et al (2021) Bio-based poly (3-hydroxybutyrate)/Thermoplastic starch composites as a host matrix for Biochar Fillers. J Polym Environ 1–14
47. Li Z, Reimer C, Wang T et al (2020) Thermal and mechanical properties of the biocomposites of Miscanthus Biocarbon and Poly (3-H ydroxybutyrate-co-3-H ydroxyvalerate)(PHBV). Polym (Basel) 12:1300
48. Ho M, Lau K, Wang H, Hui D (2015) Improvement on the properties of polylactic acid (PLA) using bamboo charcoal particles. Compos B Eng 81:14–25. https://doi.org/10.1016/j.compositesb.2015.05.048
49. Qian S, Sheng K, Yao W, Yu H (2016) Poly (lactic acid) biocomposites reinforced with ultrafine bamboo-char: morphology, mechanical, thermal, and water absorption properties. J Appl Polym Sci 133
50. Hesham M, Chamseddine G, Capucine D et al (2017) Utilization of Torrefied Coffee grounds as reinforcing Agent to produce high-quality biodegradable PBAT composites for Food Packaging Applications. ACS Sustain Chem Eng 5:1906–1916
51. Pudełko A, Postawa P, Stachowiak T et al (2021) Waste derived biochar as an alternative filler in biocomposites-Mechanical, thermal and morphological properties of biochar added biocomposites. J Clean Prod 278:123850
52. Cardoso LG, Santos JCP, Camilloto GP et al (2017) Development of active films poly (butylene adipate co-terephthalate)--PBAT

incorporated with oregano essential oil and application in fish fillet preservation. Ind Crops Prod 108:388–397
53. Abdollahi M, Damirchi S, Shafafi M et al (2019) Carboxymethyl cellulose-agar biocomposite film activated with summer savory essential oil as an antimicrobial agent. Int J Biol Macromol 126:561–568. https://doi.org/10.1016/j.ijbiomac.2018.12.115
54. Moustafa H, El-Sayed SM, Youssef AM (2021) Synergistic impact of cumin essential oil on enhancing of UV-blocking and antibacterial activity of biodegradable poly(butylene adipate-co-terephthalate)/clay platelets nanocomposites. J Thermoplast Compos Mater 36:96–117. https://doi.org/10.1177/0892705721989771
55. Guo G, Zhang C, Du Z et al (2015) Structure and property of biodegradable soy protein isolate/PBAT blends. Ind Crops Prod 74:731–736. https://doi.org/10.1016/j.indcrop.2015.06.009
56. López-Mata MA, Ruiz-Cruz S, Silva-Beltrán NP et al (2013) Physicochemical, antimicrobial and Antioxidant Properties of Chitosan Films Incorporated with Carvacrol. Molecules 18:13735–13753. https://doi.org/10.3390/molecules181113735
57. Kargarzadeh H, Galeski A, Pawlak A (2020) PBAT green composites: effects of kraft lignin particles on the morphological, thermal, crystalline, macro and micromechanical properties. Polym (Guildf) 203:122748
58. Xu Z, Qiao X, Sun K (2020) Environmental-friendly corn stover/poly (butylene adipate-co-terephthalate) biocomposites. Mater Today Commun 25:101541
59. da Costa RC, Daitx TS, Mauler RS et al (2020) Poly (hydroxybutyrate-co-hydroxyvalerate)-based nanocomposites for antimicrobial active food packaging containing oregano essential oil. Food Packag Shelf Life 26:100602
60. Cui R, Jiang K, Yuan M et al (2020) Antimicrobial film based on polylactic acid and carbon nanotube for controlled cinnamaldehyde release. J Mater Res Technol 9:10130–10138
61. Liu D, Li H, Jiang L et al (2016) Characterization of active packaging films made from poly(lactic acid)/poly(trimethylene carbonate) incorporated with oregano essential oil. Molecules 21:695–709. https://doi.org/10.3390/molecules21060695
62. Silva ID, de Andrade L, de Caetano MF VF, et al (2020) \ Development\ of\ active\ PHB/PEG\ antimicrobial\ films\ incorporating\ clove\ essential\ oil\.\ Pol\{\'\i\}Meros \ 30
63. Li G, Shankar S, Rhim J-W, Oh B-Y (2015) Effects of preparation method on properties of poly (butylene adipate-co-terephthalate) films. Food Sci Biotechnol 24:1679–1685
64. Camani PH, Souza AG, Barbosa RFS et al (2021) Comprehensive insight into surfactant modified-PBAT physico-chemical and biodegradability properties. Chemosphere 269:128708
65. de Nunes CD, de Souza E, Rosa AG (2019) D Effect of the Joncryl®ADR Compatibilizing Agent in Blends of Poly (butylene adipate-co-terephthalate)/Poly (lactic acid). In: Macromolecular Symposia. p 1800035
66. Fang S, Qiu W, Mei J, Xie J (2020) Effect of Sonication on the Properties of Flaxseed Gum Films Incorporated with Carvacrol. Int J Mol Sci 21. https://doi.org/10.3390/ijms21051637
67. Tang Y, Zhou Y, Lan X et al (2019) Electrospun Gelatin Nanofibers Encapsulated with Peppermint and chamomile essential oils as potential edible packaging. J Agric Food Chem 67:2227–2234. https://doi.org/10.1021/acs.jafc.8b06226
68. Hu X, Wang X, Li S et al (2021) Antibacterial Electrospun polyvinyl Alcohol nanofibers encapsulating berberine-Hydroxypropyl-β-cyclodextrin inclusion complex. J Drug Deliv Sci Technol 64:102649. https://doi.org/10.1016/j.jddst.2021.102649
69. Debeli DK, Wu L, Huang F (2023) PBAT-based biodegradable nanocomposite coating films with ultra-high oxygen barrier and balanced mechanical properties. Polym Degrad Stab 216:110489. https://doi.org/10.1016/j.polymdegradstab.2023.110489
70. Lopresti F, Campora S, Tirri G et al (2021) Core-shell PLA/Kef hybrid scaffolds for skin tissue engineering applications prepared by direct kefiran coating on PLA electrospun fibers optimized via air-plasma treatment. Mater Sci Engineering: C 127:112248. https://doi.org/10.1016/j.msec.2021.112248
71. Veldhuizen EJA, Tjeerdsma-van Bokhoven JLM, Zweijtzer C et al (2006) Structural requirements for the antimicrobial activity of Carvacrol. J Agric Food Chem 54:1874–1879. https://doi.org/10.1021/jf052564y
72. Tonyali B, McDaniel A, Amamcharla J et al (2020) Release kinetics of cinnamaldehyde, eugenol, and thymol from sustainable and biodegradable active packaging films. Food Packag Shelf Life 24:100484. https://doi.org/10.1016/j.fpsl.2020.100484
73. Nguyen TT, Van Giau V, Vo TK (2016) Multiplex PCR for simultaneous identification of E. Coli O157: H7, Salmonella spp. and L. monocytogenes in food. 3 Biotech 6:1–9
74. Venkatesan R, Rajeswari N (2019) Preparation, mechanical and antimicrobial properties of SiO 2/poly (butylene adipate-co-terephthalate) films for active food packaging. Silicon 11:2233–2239
75. Dhumal CV, Ahmed J, Bandara N, Sarkar P (2019) Improvement of antimicrobial activity of sago starch/guar gum bi-phasic edible films by incorporating carvacrol and citral. Food Packag Shelf Life 21:100380. https://doi.org/10.1016/j.fpsl.2019.100380
76. La Storia A, Ercolini D, Marinello F et al (2011) Atomic force microscopy analysis shows surface structure changes in carvacrol-treated bacterial cells. Res Microbiol 162:164–172
77. Cardoso LG, SILVA J, SILVA JA et al (2022) Development and characterization of antioxidant and antimicrobial poly (butylene adipate-co-terephtalate)(PBAT) film incorporated with oregano essential oil and applied in sliced mozzarella cheese. Acad Bras Cienc 94
78. Hogg S (2013) Essential microbiology, Second Edi. Wiley, Chichester